Pharm Res (2012) 29:932–942
DOI 10.1007/s11095-011-0633-0

RESEARCH PAPER

Sustained Cytoplasmic Delivery and Anti-viral Effect of PLGA Nanoparticles Carrying a Nucleic Acid-Hydrolyzing Monoclonal Antibody

Yoon Ki Joung • Sejin Son • Ji Young Jang • Myung Hee Kwon • Ki Dong Park

Received: 15 March 2011 / Accepted: 21 November 2011 / Published online: 3 December 2011

ABSTRACT

Purpose Cytoplasmic delivery of a monoclonal antibody (mAb) with nucleic acid-hydrolyzing activity (3D8 scFv) using poly(lactic-co-glycolic acid) nanoparticles (PLGA NPs) was investigated for persistent anti-viral effect.

Methods 3D8 scFv-loaded PLGA (3D8–PLGA) NPs were prepared via a double emulsion method that was previously optimized. Flow cytometry and confocal microscopy was carried out to confirm the cellular uptake and cytoplasmic localization. immunochemical and fluorescence resonance energy transfer (FRET) assays tested the cytoplasmic release and hydrolyzing effect of 3D8 scFv, respectively. Anti-viral activity test was performed using MTT assay with vesicular stomatitis virus (VSV)-infected HeLa cells.

Results 3D8–PLGA NPs were much more effectively taken into cells in dose- and time-dependent manner and localized in the cytosolic region, compared to free 3D8 scFv. 3D8 scFv was released and hydrolyzed RNAs in the cytoplasm, exhibiting the maxima at a period of time (12–24 h). Anti-viral activity test revealed that 3D8–PLGA NP has dose- and time-dependent anti-viral effect and the maximum effect at the dose of 2 mg/ml and the incubation of 3 days.

Conclusions Cytoplasmic delivery of 3D8 scFv via PLGA NPs could enhance the viability of infected cells in sustained manner due to preserved activity, much improved cellular uptake and sustained release.

KEY WORDS antiviral effect · cytoplasmic delivery · drug delivery · monoclonal antibody · nanoparticles

ABBREVIATIONS

BCA	bicinchoninic acid
BSA	bovine serum albumin
CD	circular dichroism
DMEM	dulbecco's modified eagle medium
DNA	deoxyribonucleic acid
DLS	dynamic light scattering
ELISA	enzyme-linked immunosorbent assay
FACS	fluorescence-activated cell sorter
FITC	fluorescein isothiocyanate
FRET	fluorescence resonance energy transfer
IgG	Immunoglobulin G
mAb	monoclonal antibody
MTT	3-(4,5-dimethylthiazol-2-yl)-2,5-diphenyltetrazolium bromide
PBS	phosphate buffered saline
PFA)	paraformaldehyde
PLGA	poly(lactic-co-glycolic acid)
PVA	poly(vinyl alcohol)
RNA	ribonucleic acid
SEM	scanning electron microscopy
SDS	sodium dodecyl sulphate
VSV	vesicular stomatitis virus

Yoon Ki Joung, Sejin Son and Ji Young Jang contributed equally to this work.

Y. K. Joung • S. Son • K. D. Park (✉)
Department of Molecular Science and Technology, Ajou University
San 5 Wonchon-dong, Yeongtong-Gu
Suwon 443-749, Republic of Korea
e-mail: kdp@ajou.ac.kr

J. Y. Jang • M. H. Kwon
Department of Microbiology, Ajou University School of Medicine
San 5, Wonchon-Dong, Yeongtong-Gu
Suwon 443-721, Republic of Korea

J. Y. Jang
Tumor Immunity Medical Research Center, Cancer Research Institute
Seoul National University College of Medicine
28 Yongon-dong, Jongno-gu
Seoul 110-799, Republic of Korea

Y. K. Joung
Center for Biomaterials, Korea Institute of Science and Technology
Hwarangno 14-gil 5, Seongbuk-gu
Seoul 136-791, Republic of Korea

INTRODUCTION

Anti-DNA antibodies (Abs) that are found in humans and mice with autoimmune diseases cause apoptotic cell death induced by their DNA hydrolyzing activity (1,2). Our group has investigated an anti-DNA single chain variable fragment (scFv) Ab, 3D8 scFv, which binds and hydrolyzes nucleic acids, in aspects of catalytic activities (3), crystal structure (4), mechanism of cellular uptake (5), humanization (6), and anti-viral activity (7). Consecutively, we have verified the binding and hydrolyzing activities as well as cell penetrating mechanism of 3D8 scFv (5). Nevertheless, quite short half-life and thereby low delivery efficacy makes it difficult to apply this mAb to therapeutic applications via parenteral route. Therefore, optimized formulation and delivery system are requisite for pharmaceutical applications using 3D8 scFv. However, a small number of studies have been attempted to show the therapeutic potential of recombinant proteins with anti-nucleic acid activity (2). We have formulated 3D8 scFv into a biodegradable poly(lactic-co-glycolic acid) (PLGA) nanoparticle under an optimized condition via a double emulsion method, resulting in success of formulation at the most suitable condition (8). Like other proteins, Abs may be damaged during formulation process both in liquid and solid states. The tendency to such damages depends on mainly their individual sequence, isoelectric point, hydrophobicity, and carbohydrate content (9). Based upon our previous results, our interest has been focused on the anti-viral effect of 3D8 scFv through intracellular delivery, which is induced by hydrolyzing nucleic acids produced by a virus in a virus-infected cell (7). In terms of anti-viral therapy, the therapeutic efficacy of 3D8 scFv would largely depend on the dose and duration of its availability because the site of action of 3D8 scFv should be the intracellular region (10,11). Therefore, achieving the sustained release of 3D8 scFv is key issue to improve the therapeutic efficacy. Among various nanocarriers for intracellular delivery (12,13), biodegradable nanoparticles have been gradually excluded because of invasive conditions and difficulty in preparation process (14,15). Practically, despite their familiarity, there have been rare studies in which nanoparticles of polyesters are applied to intracellular delivery (16,17). However, such studies have demonstrated sustained effect due to prolonged release time of drug (18). For instance, Panyam and coworkers reported that sustained intracellular delivery of dexamethasone using biodegradable nanoparticles resulted in a prolonged anti-proliferative effect (11). They suggested that biodegradable nanoparticles provide a useful delivery mechanism for achieving sustained cytoplasmic delivery of other therapeutic agents such as proteins, peptides, and genes.

In this study, we hypothesized that the sustained cytoplasmic release of 3D8 scFv from biodegradable polyester nanoparticles can enhance the efficacy of anti-viral therapy in which the site of drug action is cytoplasmic region. Therefore, the uptake efficiency of PLGA nanoparticles and the intracellular level of transported 3D8 scFv were investigated. In addition, nucleic acid-hydrolyzing activity of 3D8 scFv at the cytoplasm was also determined. Ultimately, the sustained anti-viral effect of 3D8-loaded PLGA nanoparticles was investigated with the cell viability of vesicular stomatitis virus (VSV)-infected HeLa cells.

MATERIALS AND METHODS

Materials

Poly(lactic-co-glycolic acid) (PLGA) (RG504H) was purchased from Boehringer Ingelheim. Micro BCA reagent kit was purchased from Pierce Biotechnology. Poly(vinyl alcohol) (PVA, 80% hydrolyzed), D-mannitol, and trypsin protease were purchased from Sigma. Sodium dodecyl sulphate (SDS) was purchased from Junsei Chemical. Plasmid Miniprep kit was purchased from Intron Inc. As fluorescent probes, fluorescein isothiocyanate (FITC) and Alexa Fluor 488 monoclonal antibody labeling kit were purchased from Invitrogen. For cell viability assay, colorimetric 3-(4,5-dimethylthiazol-2-yl)-2,5-diphenyltetrazolium bromide (MTT) was purchased from Sigma (St Louis, MO). Polyclonal rabbit anti-3D8 scFv was produced by immunization in our laboratory. TRITC-anti-rabbit IgG was obtained from Abcam (Cambridge, MA) and Hoechst 33342 was obtained from Molecular Probes (Eugene, OR).

3D8 scFv Preparation

Mouse-originated 3D8 scFv protein was bacterially expressed and purified by IgG sepharose affinity chromatography, according to previously described procedure (3). The protein concentrations were determined using extinction coefficients of 1.995 for scFv in units of mg/mL·cm at 280 nm, which were calculated from the amino acid sequence.

Preparation of 3D8–PLGA Nanoparticles

Preparation of 3D8–PLGA nanoparticles and stabilization of encapsulated 3D8 scFv were previously optimized via our method (5). Briefly, 3D8-loaded PLGA nanoparticles were prepared by using the solvent evaporation process containing the formation of multiple emulsion (w/o/w). Five hundred μg of 3D8 scFv was dissolved in 100 μL of 10 mM phosphate buffered saline (PBS, pH 7.2) and subsequently emulsified into 1 mL of PLGA in methylene chloride (50 mg/mL) by sonication (70 W, 0 cycle, Ms73 tip, 60 s) using a homogenizer (Bandelin Sonoplus, UW2070) in

an ice bath to form a primary w/o emulsion. In some emulsions, a 10% (w/v) mannitol solution was added to the aqueous phase to stabilize 3D8 scFv. Afterwards, 2 mL of external aqueous phase containing 3% (w/v) PVA as a stabilizer was added and the mixture was re-emulsified by sonication (70 W, 0 cycle, Ms73 tip, 60 s) in an ice bath. The resulting secondary w/o/w emulsion was then poured into 100 mL of a 0.3% (w/v) aqueous PVA solution under stirring with a magnetic bar to remove organic solvent. After 1 h, the nanoparticles were recovered by ultracentrifugation (Kendro Sorvall RC-5B, Langenselbold, Germany) at 15,000 g for 20 min at 4°C and washed with distilled water 5 times, followed by freeze-drying. The freeze-drying process includes freezing and drying steps. In the freezing step, washed solution of nano-emulsion was frozen at −70°C for 24 h. In the drying step, the frozen sample was dried at −30°C for 48 h. Other conditions were not available.

Characterization of 3D8–PLGA Nanoparticles

The 3D8 scFv content of PLGA nanoparticles was determined by hydrolysis method (19). Briefly, 5 mg of lyophilized nanoparticles were digested in 4 mL of a 5% sodium dodecyl sulfate (SDS) in a 0.1 N NaOH solution for 15 h at room temperature until a clear solution was obtained. The content of at least three samples was determined by a BCA protein assay. The loading amount of 3D8 scFv was determined by the BCA protein assay, which was also converted to loading efficiency. Results were presented as the encapsulation efficiency, which indicate the percentage of 3D8 scFv encapsulated in the nanoparticles with respect to the total amount of 3D8 scFv used in the process. The average diameter and the distribution of PLGA nanoparticles were measured using dynamic light scattering (DLS, FPAR-1000, Photal, Japan) equipped with a 633 nm He-Ne laser beam (scattering angle=90°) at 37°C. Samples (1 mL) were filtered through 0.45 μm syringe filters and sonicated for 10 min prior to the measurement. Average values and standard deviations of three samples were obtained for loading amount and efficiency of 3D8 scFv mAb. The freeze-dried PLGA nanoparticles were dispersed by bath-sonication in distilled water. The surface morphology of PLGA nanoparticles was observed by scanning electron microscopy (SEM). For the surface analysis, freeze-dried PLGA nanoparticles dried under vacuum for overnight and coated with gold-palladium under an argon atmosphere.

Cell Culture

Adherent human cervical cancer cell line, HeLa, HCT116, and U87MG were purchased from ATCC (Manassas, VA) and cultured in DMEM (Dulbecco's Modified Eagle Medium) supplemented with 10% (v/v) fetal calf serum, 100 units/mL penicillin, and 100 μg/mL streptomycin (Invitrogen) in a humidified 5% CO_2/95% air atmosphere at 37°C. For all experiments, low passage HeLa cells (between passage number 10 to 20) were used before treatments.

Confocal Microscopy

HeLa cells were seeded at a density of 5×10^4 cells/well in a flat-bottomed 24-well plate over a glass coverslip at 24 h before use and pre-incubated in serum-free DMEM for 30 min at 37°C, prior to the treatment of PLGA nanoparticles. Cells were incubated with 2 mg/mL PLGA nanoparticles for pre-determined times (1, 6, and 48 h) at 37°C. After stopping cellular uptake by adding three volumes of ice-cold PBS, cells were washed twice with cold PBS, fixed with 2% paraformaldehyde (PFA) in PBS for 10 min at room temperature, and then maintained to be permeable with Perm-buffer (1% BSA, 0.1% saponine, 0.1% sodium azide in PBS) for 10 min at room temperature. Cells on a coverslip were mounted in Vectashield anti-fade mounting medium (Vector Labs) and observed with a confocal microscope (Zeiss LSM 510 laser) and analyzed with an Image software (Carl Zeiss LSM).

Flow Cytometry

HeLa cells seeded at a density of 5×10^4 cells/well in a flat-bottomed 24-well plate were pre-incubated in serum-free DMEM for 30 min at 37°C and were left untreated or treated with each inhibitor for 30 min at 37°C before treatment. Suspended cells with trypsin were treated once more with 0.1%trypsin for 3 min at 37°C to wash off the surface-bound protein. After washings with ice-cold PBS once, cells were fixed and permeabilized . For FACS measurement, 3D8 scFv was labeled with Alexa Fluor 488 labeling kit (Invitrogen). PLGA nanoparticles-loaded with Alexa Fluor 488-labeled 3D8 scFv were added at various concentrations (0.1, 0.25, 0.5, and 1.0 mg/mL) to the media without a transfection agent and the cells were incubated for various times (1, 6, 12, 24, and 48 h). Cells were washed with ice-cold PBS twice, centrifuged at 50 g for 5 min under 4°C and then analyzed using a Becton Dickinson FACSCalibur™ (BD Biosciences). For each test, 1×10^4 cells were analyzed.

Determination of Intracellular 3D8 scFv Level

For the flow cytometry analysis of 3D8 scFv in the cytoplasm, HeLa cells grown in 6-well plates were pre-incubated in serum-free DMEM for 30 min at 37°C and were incubated with PLGA nanoparticles for various time periods

(from 12 h to 6 days) at 37°C. Suspended cells treated with 0.1% trypsin were treated once more with 0.1% trypsin for 3 min at 37°C to wash off the surface-bound PLGA nanoparticles. After washings with ice-cold PBS, fixed with 2% PFA in PBS for 10 min at room temperature, and then permeabilized with Perm-buffer (1% bovine serum albumin (BSA), 0.1% saponine, 0.1% sodium azide in PBS) for 10 min at room temperature. After blocking with 2% BSA in PBS for 1 h, PLGA nanoparticles-treated cells were labeled with anti-rabbit 3D8 scFv and sequentially TRITC-anti-rabbit, and then analyzed by a fluorescence activated cell sorter (FACS, FACSCalibur^{TM}, BD Biosciences).

Cytotoxicity Test

HeLa cells seeded at density of 5×10^3 cells/well in a flat-bottomed 96-well plate were cultured for 12 h at 37°C and then treated with PLGA nanoparticles with or without 3D8 scFv and native 3D8 scFv for scheduled time periods (from 1 day to 7 days) at various concentrations (from 0.1 to 2 mg/mL). Cell viability was measured by using a colorimetric MTT-based cell growth determination kit (Sigma). Cell viability was represented as the % ratio of cultured viable cells to initial control cells.

FRET-Based RNA-hydrolyzing Assay

Fluorescence resonance energy transfer (FRET)-based nucleic acid-hydrolysis assay was carried out to detect RNA-hydrolyzing activity in live cells (20). HeLa cells were cultured with 3D8 scFv (10 μM) for 2 or 24 h. Then, 21-base length of oligonucleotides labeled with 6-carboxyfluorescein (FAM) at the 5′-terminus and a black hole quencher (BHQ) at the 3′ terminus (5′ FAM - CGATGAGTGCCATGG ATATAC- BHQ 3′) was generated from M-biotech (Salt Lake City, UT). The oligonucleotides (200 nM) were delivered into HeLa cells by Lipofectamine 2000 transfection reagent grown in a black 96-well plate. Immediately after transfection, 3D8 scFv was added to the cell and the fluorescence intensity was read for 2 h and 24 h incubation in real-time by a fluorescence detector (Molecular Devices).

Anti-viral Activity Test

HeLa cells were seeded at a density of 5×10^3 cells/well in a flat-bottomed 96-well plate and grown for 24 h. The cells were pre-incubated with the serum freemedia (DMEM) for 30 min. And then nanoparticles loaded with 3D8 scFv were added at various concentrations (0.1 to 2 mg/mL, 10 μL) into the serum-free media and were incubated for various times (from 0 h to 5 days). Cells were washed with PBS and infected with VSV at 0.1 MOI. After 1 h of incubation, fresh serum DMEM (10% (v/v) fetal calf serum (FCS)), 100 units/mL of penicillin, and 100 μg/mL of streptomycin) was added. After incubation for 48 h, 20 μL of the MTT reagent was added and incubated for 4 h. The absorbance was measured with a microplate reader at 595 nm and the cell viability was calculated to be the% ratio of cell numbers in each time period per initial cell number.

Statistical Analysis

For cytotoxicity and anti-viral activity tests, data were analyzed by a Student's *t* test. P values less than 0.05 or 0.005 were considered to be statistically significant. All values are expressed as the mean ± standard deviation (S.D.).

RESULTS AND DISCUSSION

Characterizations of 3D8–PLGA Nanoparticles

In a previous study, we have reported a result of optimized formulation for retaining the stability of encapsulated 3D8 scFv (8). Specifically, a set of formulation methods has been introduced for achieving the narrow size distribution of nanoparticles, high formulation efficiency, and preserved biological activity of 3D8 scFv, which the formulation parameters contained the sonication time to produce secondary (w/o/w) emulsion, the molecular weight of PLGA, and PLGA concentration. As shown in SEM images (Fig. 1), the optimized parameters produced homogeneous PLGA nanoparticles with average sizes of 180 and 198 nm with and without mannitol, respectively (DLS data, Table I). SEM images showed not adhered and round-shaped nanoparticles with relatively regular sizes. In addition, one of the key parameters obtained from our experience was to add mannitol as an additive for the preservation of 3D8 scFv stability, which was demonstrated by various evaluations containing circular dichroism (CD), fluorescence spectroscopy, ELISA, and agarose gel electrophoresis (data not shown). Although the addition of mannitol changed the result of formulation, little changes were exhibited (Table I). The presence of mannitol in emulsions little reduced the formulation efficiency and particle size. In addition, the surface charge of PLGA nanoparticles was tested and presented in Table I. In some literatures, the surface charge of PLGA particles was showed at a range from −10 to −35 mV, which is good agreement with our result (around −24 mV) (19,22,24). It is reported that PLGA nanoparticles rapidly escape the endo-lysosomal compartment because of their negative charge opposite to positive the compartment (22).

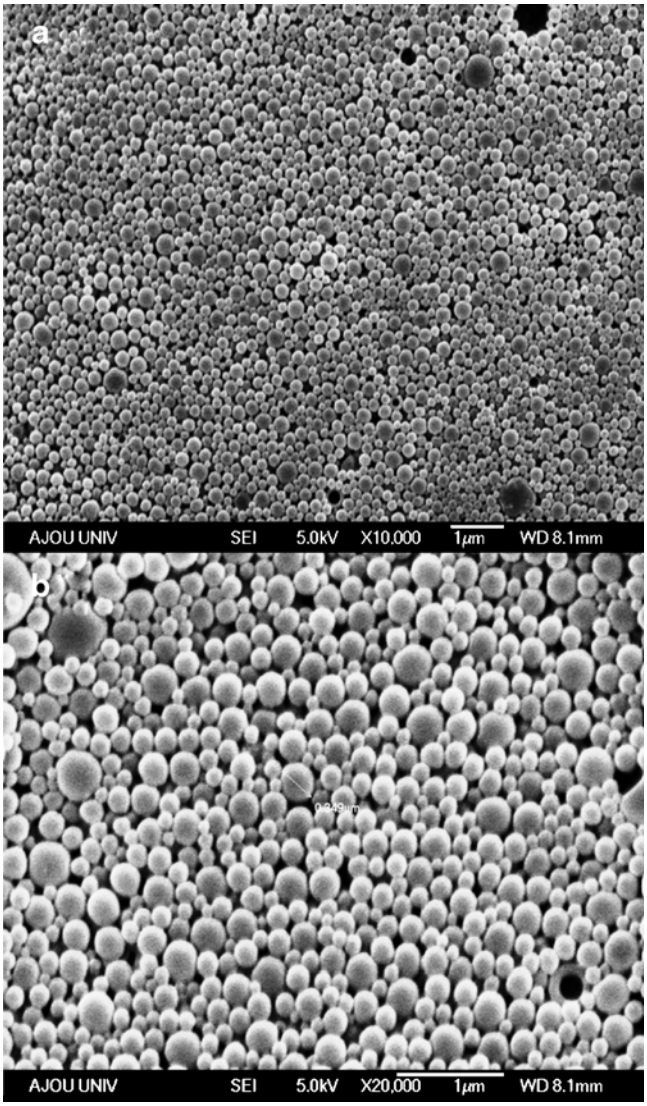

Fig. 1 Scanning electron microscopic images of 3D8–PLGA nanoparticles prepared by a w/o/w double emulsion method.

Intracellular Uptake and Distribution of 3D8–PLGA Nanoparticles

FACS analysis was conducted to observe quantitatively the cellular uptake of PLGA nanoparticles into HeLa cells. Figure 2 shows the influence of incubation time and nanoparticle concentration on the cellular uptake of PLGA nanoparticles into human cervical cancer HeLa cells. The uptake level increased in the concentration-dependent manner up to 2 mg/mL when HeLa cells were treated with PLGA nanoparticles for 12 h (Fig. 2b). In the case in which HeLa cells were treated with 2 mg/mL of PLGA nanoparticles for 48 h, the uptake level almost reached the maximum level after 12 h of incubation (Fig. 2a). From this result, the dose of 2 mg/mL and the incubation time of 12 h were considered as an optimal condition for anti-virus therapy.

Table I The Effect of Mannitol Addition as an Additive on Formulation Efficiency and Hydrodynamic Size

Mannitol	Diameter (nm)[a]	Loading amount (μg/mg)[a]	Loading efficiency (%)	Zeta-potential (mV)
+	180 ± 21	10.5 ± 0.08	65 ± 0.5	−24.5 ± 1.3
−	198 ± 14	9.6 ± 0.04	89 ± 0.4	−25.8 ± 0.4

[a] mean ± S.D. (n=3)

We investigated once again the internalization of PLGA nanoparticles into cells using confocal microscopy (Fig. 3). Naked FITC–3D8 scFv in solution (1 μM/plate) equivalent to the dose loaded in nanoparticles as a control group and blank PLGA nanoparticles (2 mg/mL) were also applied to a separate group. As shown in Fig. 3a, when HeLa cells treated with 2 mg/mL of 3D8–PLGA nanoparticles at various incubation times, the area of red fluorescence gradually increased in the HeLa cells up to 48 h. The increased area of red fluorescence indicates that most of Alexa–PLGA nanoparticles are localized in the cytoplasmic compartment. After 1-h incubation, nanoparticles were accumulated near the cellular membrane, and then moved toward nucleus, indicating that a majority of nanoparticles may be present either in late endosomes/lysosomes or in the cytoplasm. On the contrary, in the case in which HeLa cells were treated with naked FITC–3D8 scFv (Fig. 3b), though it exhibited green fluorescence at 6 h, the intensity was significantly reduced at 48 h. This means that naked 3D8 scFv was transiently localized in the cytoplasm.

Based on confocal microscopic images, the intracellular localization of PLGA nanoparticles and released 3D8 scFv were similar in the cytoplasmic compartment at 1 h incubation. And the stronger red fluorescence of PLGA nanoparticles than released 3D8 scFv was observed. But the differences in the intracellular distribution and localization of PLGA nanoparticles compared to free 3D8 scFv began to be observed after 6 h incubation. Interestingly, in contrast to gradual reduction of red fluorescence of PLGA nanoparticles, green fluorescence of released 3D8 scFv is gradually prominent as the incubation time increases. Moreover, while increasing the incubation time, the green fluorescence of released 3D8 scFv appeared near nucleus, suggesting different trafficking from that of PLGA nanoparticles.

To achieve successful intracellular delivery, delivery systems must be efficiently internalized into the cells and then localized in the cytoplasmic compartment rather than be retained in the endo-lysosomal compartment (21). Panyam *et al.* have reported that nanoparticles could release the encapsulated drug slowly when those were retained in cytosolic regions (22). This induced sustained release of a drug, which was especially crucial for protein drugs susceptible to be degraded by protease. They also

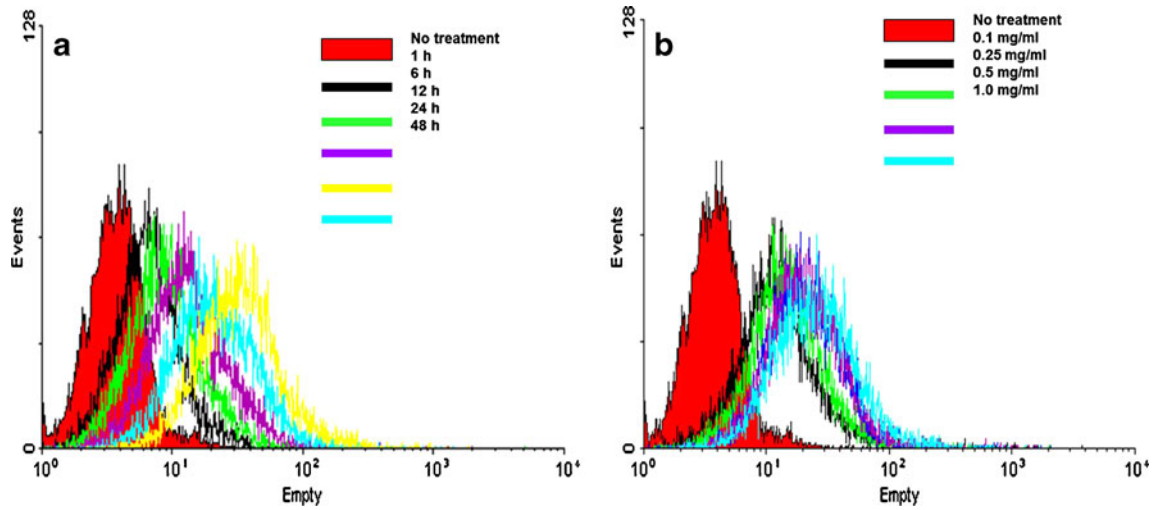

Fig. 2 Flow cytometric analysis of HeLa cells that were cultured (**a**) at the concentration of 2 mg/mL for different incubation times (1, 6, 12, 24, and 48 h) and (**b**) at different concentrations (0.1, 0.25, 0.5, and 1.0 mg/mL) of 3D8–PLGA nanoparticle for 12 h. Alexa Fluor 488-labeled 3D8 scFv was encapsulated into PLGA nanoparticles.

suggested that biodegradable nanoparticles could offer a potentially useful delivery mechanism for achieving sustained cytoplasmic delivery of therapeutic agents such as proteins, peptides, and genes. On the basis of these facts, we hypothesized that the sustained cytoplasmic release of 3D8 scFv from nanoparticles also could potentiate 3D8 scFv of which the site of action is the cytoplasmic region in terms of anti-virus therapy. Preferentially, confocal microscopy and flow cytometry were carried out to elucidate the hypothesis. For the purpose, Alexa–PLGA nanoparticles and FITC–3D8 scFv was prepared. Confocal images of HeLa cells treated with fluorescence-labeled samples demonstrated that PLGA nanoparticles were internalized from the early stage of incubation after the treatment. This tendency was

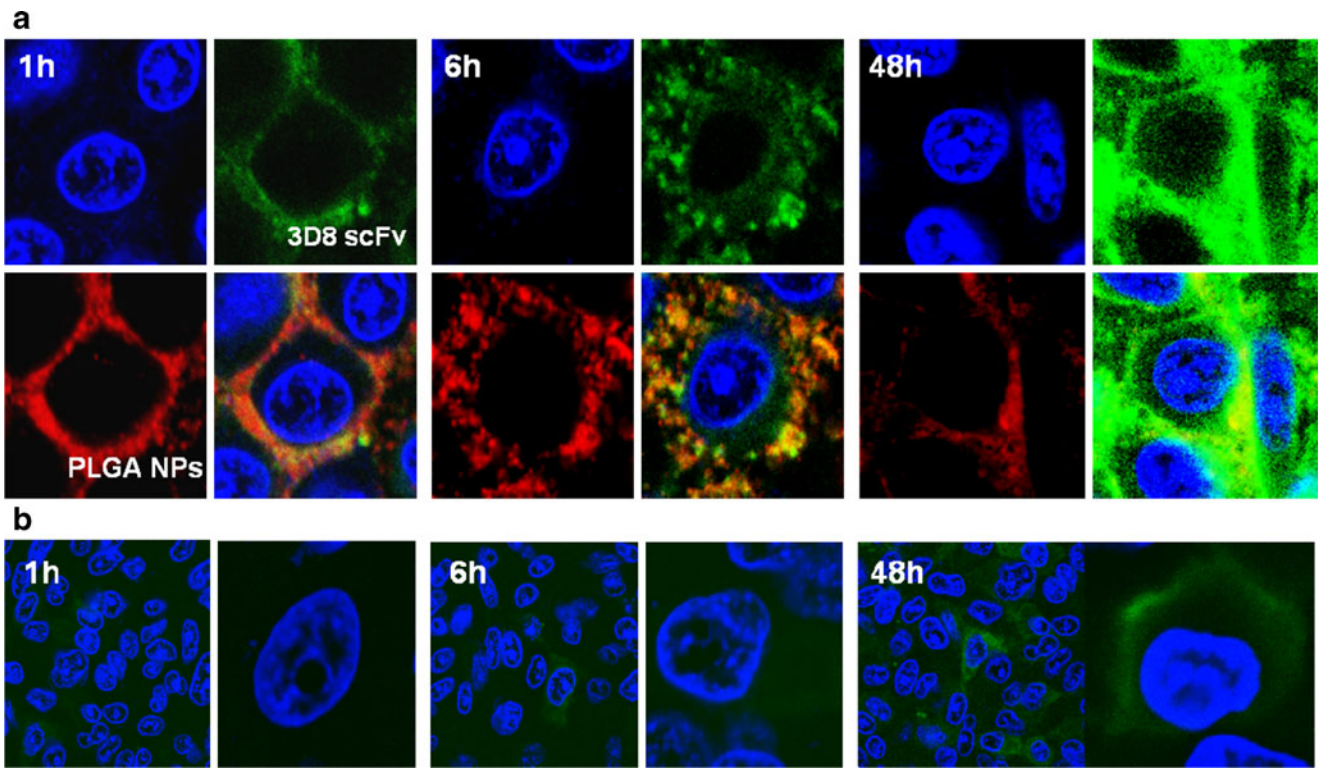

Fig. 3 Time-course study of the intracellular uptake and retention of 3D8–PLGA nanoparticle (**a**) and naked 3D8 scFv (**b**). HeLa cells were transfected with either 1 μM naked 3D8 scFv labeled with FITC (*green*) or Alexa Fluor 488-conjugated PLGA nanoparticles (*red*). The nuclei were stained with DAPI (*blue*).

also confirmed quantitatively by FACS analysis. Practically, the uptake level of PLGA nanoparticles is most likely to reach almost the plateau within 12 h. On the other hand, although most of anti-DNA mAbs including 3D8 scFv are known to be internalized into many cells, the cellular uptake of naked 3D8 scFv was relatively insignificant. From these results, it is clearly demonstrated that the formulation of 3D8 scFv into PLGA nanoparticles is efficient for intracellular delivery. The experiment for confirming the intracellular pathway of 3D8-PLGA nanoparticle was not performed in this study. But the pathway seems to depend on the nature of PLGA nanoparticle. A Previous reference suggested that PLGA nanoparticles were internalized by vascular smooth muscle cells (VSMCs) via energy-dependent endocytic pathways including adsorptive fluid phase pinocytosis (22).

3D8 scF Release from PLGA Nanoparticles in the Cytoplasm

The confocal microscopic observations of sustained intracellular 3D8 scFv levels released from PLGA nanoparticles were further confirmed using a quantitative method. To investigate the correlation between the amount of released 3D8 scFv and therapeutic efficacy, various doses of 3D8–PLGA nanoparticles with different amounts of 3D8 scFv were prepared and investigated (Fig. 4), but we selected 2 mg/mL sample because of the lower limitation of detection. Intracellular 3D8 scFv levels were rapidly increased after 12 h incubation and almost saturated at 24 h. However, the intracellular level of 3D8 scFv decreased transiently at 2 days. After that, their intracellular levels were maintained until 6 days. This result may be explaned by comparing with results in confocal microscopy and flow cytometry. It is still not clear that PLGA nanoparticles have the sustained release effect of 3D8 scFv within cells and thereby the period of action is retained for a longer time. In the confocal microscopic data, although transiently increased fluorescence was observed at 48 h, it is still not reliable because of following reason (22). When FITC was conjugated to 3D8 scFv, the actual intracellular level of released 3D8 scFv is difficult to be determined. That is because fluorescence-labeled molecules entrapped in nanoparticles could not be detected by flow cytometry and confocal microscopy. Therefore, immunocytochemical analysis was applied to determine selectively released 3D8 scFv from PLGA nanoparticles in the cytoplasm. When anti-3D8 scFv was treated to cells, internalized 3D8 scFv could associate with only 3D8 scFv released in the cytoplasm. At two incubation periods (12 and 24 h), the levels were the maximum and quite lower levels were maintained before and after those time points up to 6 days. The similar sustained cytosolic release profile has been observed in a study utilizing PLGA nanoparticles encapsulated with plasmid DNA (23). The study showed that red fluorescence-labeled plasmid DNA was internalized in almost all of cells, as shown in this study, but the intracellular release rate was little slower than our case. Also, it may be elucidated that this result is attributed to the surface charge of PLGA nanoparticles. In other studies, it has been demonstrated that selective surface charge opposite to the acidic endo-lysosomes facilitates endo-lysosomal escape of PLGA nanoparticles and delivers their payload in the cytoplasm at relatively slower rate of release, leading to a sustained therapeutic effect (22,24). In our confocal results, this tendency was observed. In the early stage of the treatment, PLGA nanoparticles were localized near cell membrane (1 h), and then entirely dispersed in a shape of spot (6 h), indicating that PLGA nanoparticles were confined in endo-lysosomes. Finally, the fluorescence was partially faded out (48 h).

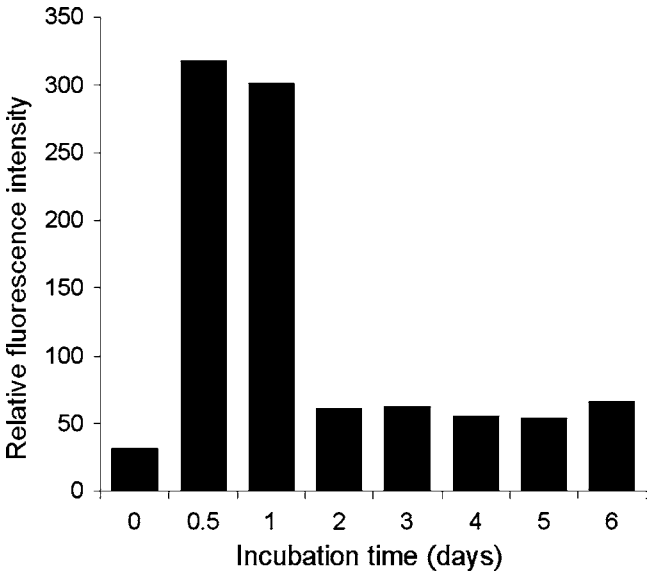

Fig. 4 Relative fluorescence intensities of intracellularly internalized 3D8 scFv that was released from PLGA nanoparticles with incubation time. 3D8 scFv in cytoplasm was visualized by immunocytochemical method using FITC-labeled anti-3D8 scFv antibody.

Cytotoxicity of 3D8–PLGA Nanoparticles

The viability of HeLa cells treated with 3D8–PLGA nanoparticles exhibited significant differences depending on concentration and incubation time (Fig. 5). As shown in Table I, 3D8-PLGA nanoparticle was prepared at a condition with mannitol addition and the loading amount was 10.5 μg/mg. The amount of naked 3D8 scFv was adjusted to that of 3D8 scFv loaded into 3D8-PLGA nanoparticle. PLGA nanoparticles showed lower cytotoxicity than 3D8–PLGA nanoparticles at all concentrations and incubation times. In the case of 3D8–PLGA nanoparticles, the cell viability reduced as increasing the concentration of 3D8–PLGA nanoparticles. Free 3D8 scFv also had cytotoxic

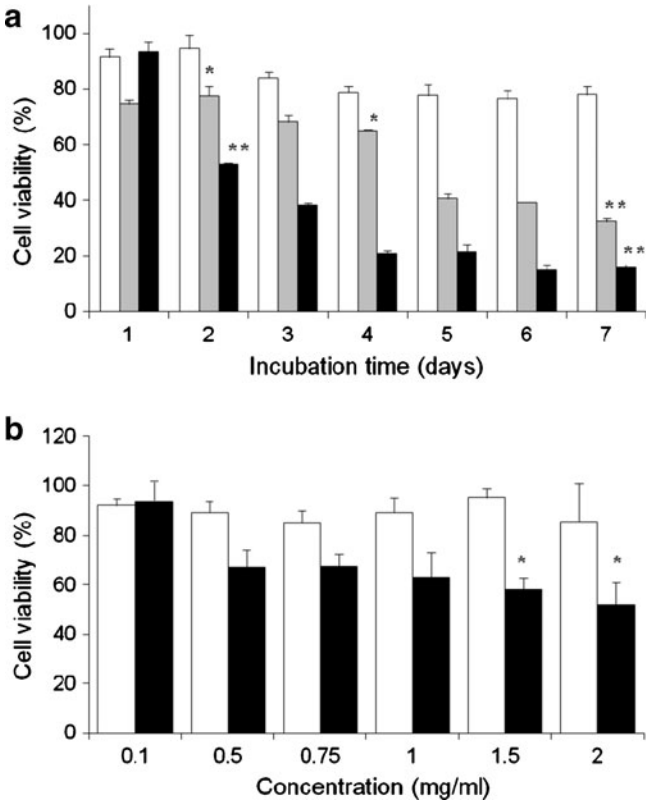

Fig. 5 Dose- and time-dependent cytotoxicity of free 3D8 scFv (*gray bar*), 3D8–PLGA nanoparticles (*black bar*) and blank PLGA nanoparticles (*white bar*): (**a**) HeLa cells were incubated with 2 mg/mL nanoparticles and 1 μM native 3D8 scFv at various time intervals (from 1 to 7 days) and (**b**) incubated at various nanoparticle concentrations (from 0.1 to 2 mg/mL) for 48 h. Cell viability was measured with MTT assay; Mean ± S.D. (n=3)*, $P<0.05$; **, $P<0.005$ (*versus* blank PLGA nanoparticles, by Student's t test.)

effect on HeLa cells, which self-internalization and its mechanism of 3D8 scFv has been reported by our group. Obtained results demonstrated that PLGA nanoparticle itself has slight cytotoxicity and 3D8 scFv acts on the inhibition of cell growth, of which the action is enhanced by PLGA nanoparticles.

To confirm the accuracy of results, the intracellular level of 3D8 scFv needs to be correlated with cytotoxicity result. From determined intracellular levels of 3D8 scFv, we could estimate that the amount of 3D8 scFv released from PLGA nanoparticles was the maximum up to 1 day. However, the cytotoxic effect was presented after 2 days and gradually increased. In time-kinetics of 3D8 scFv delivery, the profile of intracellular level is evidently different from that of cytotoxicity. This difference presumably resulted from the temporal gap between the cytoplasmic existence and the induction of cytotoxic effect. 3D8–PLGA nanoparticle seems to have comparatively sustained cytotoxic effect even up to 7 days, compared to other types of nanocarriers based on polymers, such as liposomes (25), micelles (26–28), polyion complexes (29), and gel-like structures (30,31).

RNA Hydrolyzing Activity of 3D8 scFv in the Cytoplasm

FRET-based cleavage assay was performed to evaluate the RNA-hydrolyzing activity of 3D8 scFv localized in the cytosolic region of HeLa cell, which determines the hydrolysis of the transfected RNAs that are double-labeled with a fluorophore at 5′-terminus and its quencher at 3′-terminus. HeLa cells were incubated with 3D8–PLGA nanoparticles at several time points for 48 h, prior to transfection of double-labeled RNA substrate, and the intensity of fluorescence in cells was measured in real-time with 5-minute intervals for 2 h by a fluorescence analyzer (shown in Fig. 6). The fluorescence intensity of 3D8 scFv-treated samples was higher than that of untreated samples over the detection time, which demonstrated RNA-hydrolyzing activity of 3D8 scFv in the cytosol. More importantly, the activity of 3D8 scFv internalized by PLGA nanoparticle was higher than that of 3D8 scFv only. The activity of 3D8 scFv was confirmed via some experiments such as cytotoxicity, hydrolyzing activity, and antiviral activity. The influence of PLGA nanoparticle was also evaluated in the cytotoxicity and antiviral activity tests. The result demonstrated that the effect of PLGA nanoparticle on cytotoxicity and antiviral effect is not significant. In this experiment, we aimed at investigating nucleic hydrolyzing activity of 3D8 scFv especially in the cytoplasm by FRET assay. Although the 3D8 scFv that was internalized into the cell showed the activity, there were no differences in the activity between naked and particle-delivered 3D8 scFv after 12-h incubation. This result probably attributed to the sustained release rate of 3D8 scFv from PLGA nanoparticles.

Our group has reported nucleic acids-binding and -hydrolyzing activities of 3D8 scFv (3). When 3D8 scFv was once internalized into a cell, this bound and hydrolyzed all cytoplasmic nucleic acids including DNAs and RNAs because it does not have sequence-specificity, ultimately inducing cytotoxic effect.

More specifically, practical actions of 3D8 scFv derived from its nucleic acid-hydrolyzing activity were investigated under the cytoplasmic environment by using FRET analysis. 3D8–PLGA nanoparticles show high hydrolyzing activity at all time points. 3D8 scFv also had similar activity after 12 h, though it was little lower than 3D8–PLGA nanoparticles before 12 h. This fact indicates that 3D8 scFv actually act as a nuclease at a sustained manner, like our expectation, but PLGA nanoparticles little influenced the enhancement of the activity, contrary to our expectation.

Anti-viral Activity

Therapeutic availability of 3D8 scFv via intracellular delivery for anti-viral therapy was evaluated by the infection of

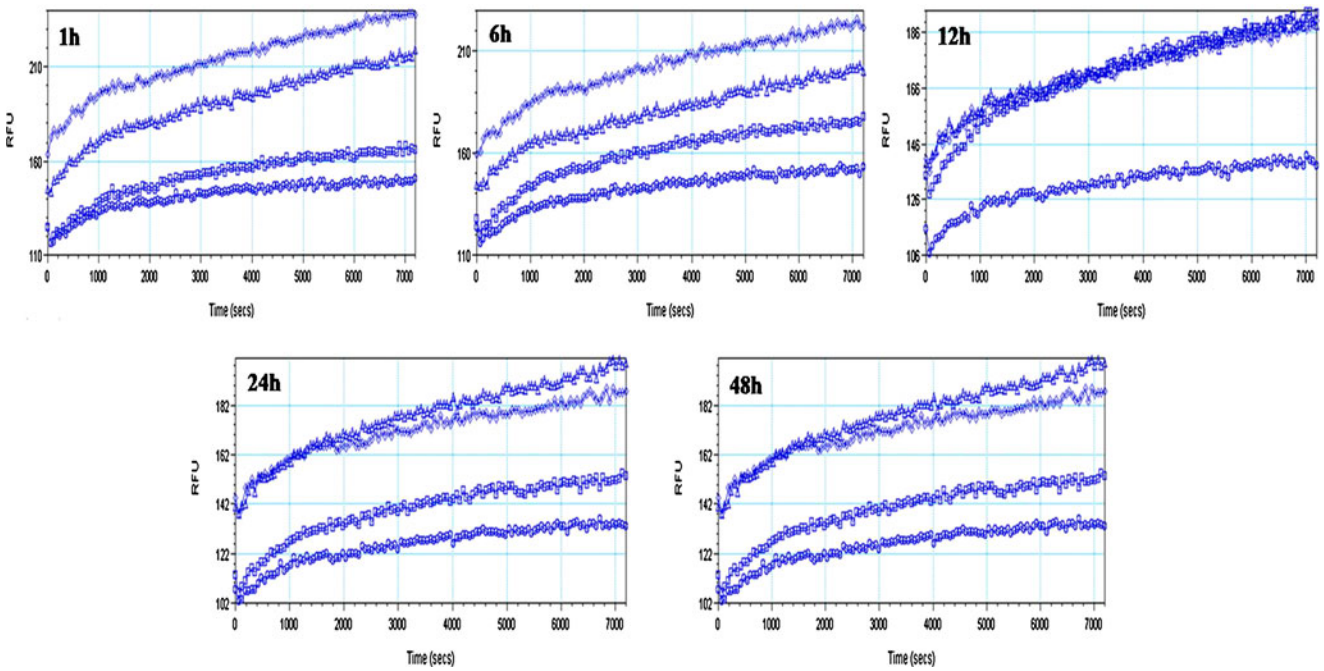

Fig. 6 Anti-RNA activity of cytosolic 3D8 scFv released from PLGA nanoparticles in HeLa cell, measured by FRET assay. Treated samples include DL-RNA (*circle*), PLGA + DL-RNA (*square*), 3D8 + DL-RNA (triangle), and 3D8–PLGA + DL-RNA (*diamond*).

cells with vesicular stomatitis virus (VSV) as shown in Fig. 7. At 12 h after treating cells with 3D8–PLGA nanoparticles, 0.1 MOI of VSV was treated for 1 h and thereafter the cell viability was determined at different nanoparticle concentrations for 48 h by MTT assay. Drug-free PLGA nanoparticles were also treated as a control at the same time. Among the various concentrations (0.1–2 mg/mL) of 3D8–PLGA nanoparticles, the treatment of 2 mg/mL was most efficacious for healing virus-infected cells, demonstrated by significantly increased cell viability. To confirm the long-term efficacy of 3D8 scFv induced by PLGA degradation, cell viability was further evaluated up to 6 days by treating with 2 mg/mL of 3D8 scFv. The result shows that the cell viability is maintained by 3 days but decreased for 3 days after that time. We have evaluated the antiviral activity of 3D8 scFv in the previous study (7). This study similarly showed naked 3D8 scFv had anti-nucleic acids activity and cytotoxicity.

As a therapeutic model of 3D8 scFv, anti-viral study is one of most suitable applications because the site and period of action of 3D8 scFv most coincides with sustained cytoplasmic delivery. Therefore, we verified that 3D8 scFv is internalized into cells via caveolae-mediated endocytosis and thereafter localized in the cytosol (5). Moreover, it is also demonstrated that 3D8 scFv has antiviral activity against classical swine fever virus. However, it is still needed to enhance the efficacy for therapeutic availability (7). For this purpose, 3D8 scFv was formulated with biodegradable PLGA nanoparticle that is degraded by hydrolysis in the sustained manner. The cellular activities of 3D8 scFv have been verified by our continuous studies. Moreover, the formulation has been also guaranteed by optimizing various processing parameters in our previous work (8). Ultimately, the first trial of 3D8 scFv delivery in an *in vitro* virus-infection model was fairly encouraged. Furthermore, the results that analyzed anti-RNA and anti-viral activities were well correlated with those of the intracellular determination and the cytotoxicity of 3D8 scFv. Anti-viral activity study demonstrated that anti-viral activity of 3D8 scFv was most likely very efficacious over a critical concentration, which was exhibited at 2 mg/mL in this study, and the sustained effect of anti-viral activity was shown for 3 days and fallen after that but maintained up to 6 days. Considering the cytotoxicity result (Fig. 5), anti-viral activity is probably able to be improved by modulating treatment dose or loading amount. However, the regulation of the effective dose for its therapeutic use without cytotoxicity, with maintaining its biological activity, seems to be very difficult. This difficulty has been a major hurdle to utilize PLGA-based nanoparticles as a protein delivery platform, especially in case of intracellular delivery in spite of their promising merit potentiating the sustained therapeutic efficacy. To the best of our knowledge, we could almost not find any kind of reports about intracellular protein delivery using biodegradable polymeric nanoparticles for their therapeutic activity like this study. For further study, immunogenicity and efficacy in animal models should be investigated.

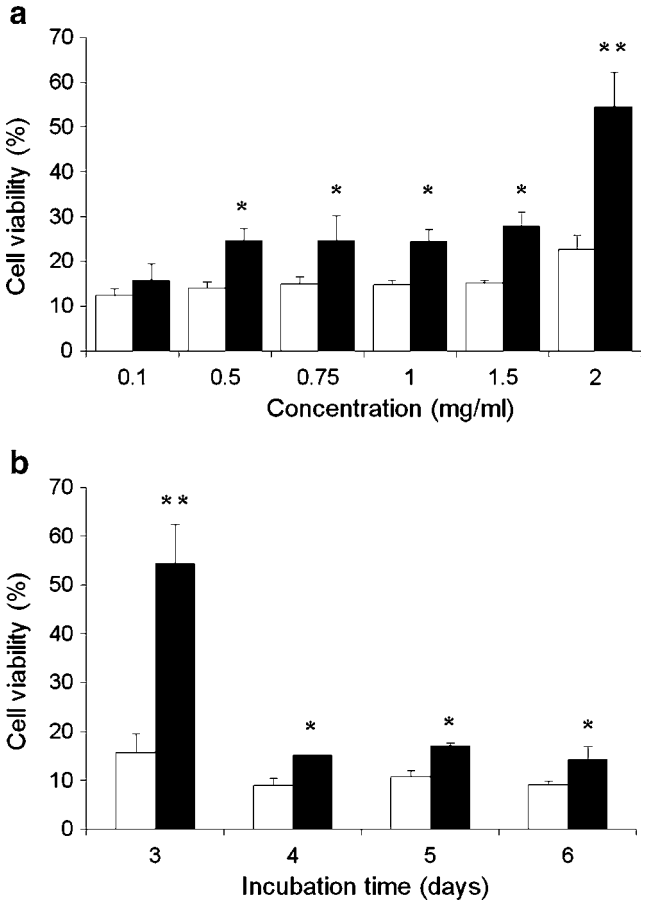

Fig. 7 Antiviral activity of 3D8 scFv released from PLGA nanoparticles in HeLa cell in aspects of (**a**) dose and (**b**) pre-incubation time kinetics of 3D8-loaded PLGA nanoparticles (black bar) and blank PLGA nanoparticles (*white bar*). Cell viability was measured with MTT assay. Mean ± S. D. ($n=3$). *, $P<0.05$; **, $P<0.005$ (*versus* blank PLGA nanoparticles, by Student's *t* test).

CONCLUSION

Using optimized 3D8–PLGA nanoparticles for intracellular delivery, our studies showed that intracellular release of 3D8 scFv from PLGA nanoparticles was sustained for at least 6 days. Further, intracellular levels of 3D8 scFv was well correlated with and the anti-virus activity. Conclusively, based on these comprehensive analyses including intracellular 3D8 scFv level, cytotoxicity and anti-virus activity tests demonstrate that the confirmed intracellular levels and practical nucleic acid-hydrolyzing activity of 3D8 scFv induced considerably and potentially high anti-virus activity. This study hopefully suggests the feasibility and rationale that anti-nucleic acid hydrolyzing mAbs can be formulated with biodegradable nanoparticles and applied to cytoplasmic delivery applications including anti-virus therapies, requiring a sustained therapeutic effect.

ACKNOWLEDGMENTS & DISCLOSURES

This research was supported by grants from the Fundamental R&D Program for Core Technology of Materials funded by the Ministry of Knowledge Economy, Republic of Korea (K0006028) and Priority Research Centers Program through the National Research Foundation of Korea (NRF), Ministry of Education, Science and Technology, Republic of Korea (2009–0093826).

REFERENCES

1. Marion TN, Krishnan MR, Desai DD, Jou NT, Tillman DM. Monoclonal anti-DNA antibodies: structure, specificity, and biology. Methods. 1997;11:3–11.
2. Jang YJ, Stollar BD. Anti-DNA antibodies: aspects of structure and pathogenicity. Cell Mol Life Sci. 2003;60:309–20.
3. Kim YR, Kim JS, Lee SH, Lee WR, Sohn JN, Chung YC, Shim HK, Lee SC, Kwon MH, Kim YS. Heavy and light chain variable single domains of an anti-DNA binding antibody hydrolyze both double- and single-stranded DNAs without sequence specificity. J Biol Chem. 2003;281:15287–95.
4. Park SY, Lee WR, Lee SC, Kwon MH, Kim YS, Kim JS. Crystal structure of single-domain VL of an anti-DNA binding antibody 3D8 scFv and its active site revealed by complex structures of a small molecule and metals. Proteins. 2091–2096.
5. Jang JY, Jeong JG, Jun HR, Lee SC, Kim JS, Kim YS, Kwon MH. A nucleic acid-hydrolyzing antibody penetrates into cells via caveolae-mediated endocytosis, localizes in the cytosol and exhibits cytotoxicity. Cell Mol Life Sci. 2009;66:1985–97.
6. Kim DS, Lee SH, Kim JS, Lee SC, Kwon MH, Kim YS. Generation of humanized anti-DNA hydrolyzing catalytic antibodies by complementarity determining region grafting. Biochem Biophys Res Comm. 2009;379:314–8.
7. Jun HR, Pham CD, Lim SI, Lee SC, Kim YS, Park S, Kwon MH. An RNA-hydrolyzing recombinant antibody exhibits an antiviral activity against classical swine fever virus. Biochem Biophys Res Comm. 2010;395:484–9.
8. Son S, Lee WR, Joung YK, Kwon MH, Kim YS, Park KD. Optimized stability retention of a potential monoclonal antibody for the encapsulation into PLGA nanoparticles. Int J Pharm. 2009;368:178–85.
9. Bogard WC, Dean RT, Deo Y, Fuchs R, Mattis JA, McLean AA, Berger HJ. Practical considerations in the production, purification, and formulation of monoclonal antibodies for immunoscintigraphy and immunotherapy. Semin Nucl Med. 1989;19:202–20.
10. Suh H, Jeong B, Rathi R, Kim SW. Regulation of smooth muscle cell proliferation using paclitaxel-loaded poly(ethylene oxide)-poly(lactide/glycolide) nanospheres. J Biomed Mater Res. 1998;42:331–8.
11. Panyam J, Labhasetwar V. Sustained cytoplasmic delivery of drugs with intracellular receptors using biodegradable nanoparticles. Mol Pharmaceut. 2004;1:77–84.
12. Jianga W, Guptab RK, Deshpandec MC, Schwendemanc SP. Biodegradable poly(lactic-co-glycolic acid) microparticles for injectable delivery of vaccine antigens. Adv Drug Deliv Rev. 2005;57:391–410.
13. Hanesa J, Clelandb JL, Langer R. New advances in microsphere-based single-dose vaccines. Adv Drug Deliv Rev. 1997;28:97–119.

14. Haidara ZS, Hamdy RC, Tabrizian M. Protein release kinetics for core–shell hybrid nanoparticles based on the layer-by-layer assembly of alginate and chitosan on liposomes. Biomaterials. 2008;29:1207–15.
15. Wei L, Cai C, Lin J, Chen T. Dual-drug delivery system based on hydrogel/micelle composites. Biomaterials. 2009;30:2606–13.
16. Soppimatha KS, Aminabhavia TM, Kulkarnia AR, Rudzinski WE. Biodegradable polymeric nanoparticles as drug delivery devices. J Control Release. 2001;70:1–20.
17. Chana JM, Zhang L, Yuet KP, Liao G, Rheed JW, Langer R, Farokhzad OC. PLGA–lecithin–PEG core–shell nanoparticles for controlled drug delivery. Biomaterials. 2009;30:1627–34.
18. Fay F, Quinn DJ, Gilmore BF, McCarron PA, Scott CJ. Gene delivery using dimethyldidodecylammonium bromide-coated PLGA nanoparticles. Biomaterials. 2010;31:4214–22.
19. Hora HS, Rana RK, Nunberg JH, Tice TR, Gilley RM, Hudson ME. Release of human serum albumin from poly (lactide-co-glycolide)microspheres. Pharm Res. 1990;7:1190–4.
20. Townsend HL, Jha BK, Han J, Maluf NK, Silverman RH, Barton DJ. A viral RNA competitively inhibits the antiviral endoribonuclease domain of RNase L. RNA. 2008;14:1026–36.
21. Sahoo SK, Labhasetwar V. Enhanced antiproliferative activity of transferrin-conjugated paclitaxel-loaded nanoparticles is mediated via sustained intracellular drug retention. Mol Pharmaceut. 2005;2:373–83.
22. Panyam J, Zhou WZ, Prabha S, Sahoo SK, Labhasetwar V. Rapid endo-lysosomal escape of poly(DL-lactide-co-glycolide) nanoparticles: implications for drug and gene delivery. FASEB J. 2002;16:1217–26.
23. Prabha S, Labhasetwar V. Nanoparticle-mediated wild-type p53 gene delivery results in sustained antiproliferative activity in breast cancer cells. Mol Pharmaceut. 2004;1:211–9.
24. Vasir JK, Labhasetwar V. Biodegradable nanoparticles for cytosolic delivery of therapeutics. Adv Drug Deliv Rev. 2007;59:718–28.
25. Tan ML, Choong PFM, Dass CR. Recent developments in liposomes, microparticles and nanoparticles for protein and peptide drug delivery. Peptides. 2010;31:184–93.
26. Liu Z, Jiao Y, Wang Y, Zhou C, Zhang Z. Polysaccharides-based nanoparticles as drug delivery systems. Adv Drug Deliv Rev. 2008;60:1650–62.
27. Joung YK, Bae JW, Park KD. Controlled release of heparin-binding growth factors using heparin-containing particulate systems for tissue regeneration. Expert Opin Drug Deliv. 2008;5:1173–84.
28. Lee JS, Go DH, Bae JW, Lee SJ, Park KD. Heparin conjugated polymeric micelle for long-term delivery of basic fibroblast growth factor. J Control Release. 2007;117:204–9.
29. Reddy PD, Swarnalatha D. Recent advances in novel drug delivery systems. Int J PharmTech Res. 2010;2:2025–7.
30. Joung YK, Lee JS, Lee SJ, Park KD. 6-Arm PLLA-PEG block copolymers for micelle formation and controlled drug release. Macromol Res. 2008;16:66–9.
31. Lee JS, Bae JW, Joung YK, Lee SJ, Han DK, Park KD. Controlled dual release of indomethacin and basic fibroblast growth factor from heparin-conjugated polymeric micelle. Int J Pharm. 2008;346:57–63.